

# Polar nephelometer for light-scattering measurements of ice crystals

B. Barkey and K. N. Liou

*Department of Atmospheric Sciences, University of California, Los Angeles, Los Angeles, California 90095*

Received September 11, 2000

We report on a small, lightweight polar nephelometer for the measurement of the light-scattering properties of cloud particles, specifically designed for use on a balloonborne platform in cirrus cloud conditions. The instrument consists of 33 fiber-optic light guides positioned in a two-dimensional plane from  $5^\circ$  to  $175^\circ$  that direct the scattered light to photodiode detectors–amplifier units. The system uses an onboard computer and data acquisition card to collect and store the measured signals. The instrument's calibration is tested by measurement of light scattered into a two-dimensional plane from small water droplets generated by an ultrasonic humidifier. Excellent comparisons between the measured water-droplet scattering properties and expectations generated by Mie calculation are shown. The measured scattering properties of ice crystals generated in a cold chamber also compare reasonably well with the theoretical results based on calculations from a unified theory of light scattering by ice crystals that use the particle size distribution measured in the chamber.

© 2001 Optical Society of America

OCIS codes: 010.1310, 290.1090, 290.5820, 290.5850.

Cirrus clouds are composed of ice crystals that generally have hexagonal shapes that vary in both time and space from simple plates and columns to complex hexagonal shapes, such as aggregates and bullet rosettes. The manner in which sunlight interacts with ice crystals is dependent on the crystals' size, shape, and orientation with respect to the incident light direction. In recent years, through theoretical and numerical efforts, it has become possible to determine the scattering-phase function of these nonspherical ice particles,<sup>1–3</sup> which describes the three-dimensional single-scattering intensity distribution. The scattering-phase functions are highly dependent on the crystal habit and orientation. For remote-sensing applications, it is imperative to have proper phase-function information to develop reliable methods for the retrieval of the optical and microphysical properties of ice clouds, based on bidirectional reflectance measurements from space.<sup>4</sup> We have designed an instrument for the purpose of measuring the scattering properties in a two-dimensional plane of ice crystals that occur in the atmosphere.

Polar nephelometers have been used to measure the scattering properties of ice-cloud particles in a laboratory setting.<sup>5,6</sup> Successful use of nephelometers in aircraft has been limited.<sup>7,8</sup> It is our intent to develop an instrument that one can use on a balloonborne platform to prevent the uncertainties inherent in the scattering measurements of aircraft-based instruments, which are caused by the high speed of the aircraft. Also, since the instrument measures the scattering properties of freely falling particles, information caused by any preferred crystal orientation could be preserved.

As shown in Fig. 1, there are 33 fiber-optic light guides positioned to sense the light that is scattered from particles in a two-dimensional plane from  $5^\circ$  to  $175^\circ$ . The angular displacement of the fiber optics is reduced between  $20^\circ$  to  $25^\circ$  and between  $120^\circ$  and

$170^\circ$ . The fiber light guides have a diameter of 1 mm, and, given the array diameter of 15 cm, each fiber light guide collects a solid angle of approximately  $1.4 \times 10^{-4}$  sr. A 3-mm-diameter collimated and unpolarized spherical beam from a small diode laser with a wavelength of 670 nm and a power of 0.95 mW illuminates the scattering sample, which is allowed to fall freely into the center of the fiber-optic sensor array through a small black aluminum tube with an inside diameter of 3 mm. A larger black aluminum tube (5-mm inside diameter) directs the falling crystals out of the bottom of the instrument. The amount of unwanted scattered light in the scattering volume is minimal because of a beam dump that prevents the laser beam from backscattering into the detector array and two three-dimensional light absorbers that are positioned above and below the scattering plane to absorb light that is scattered

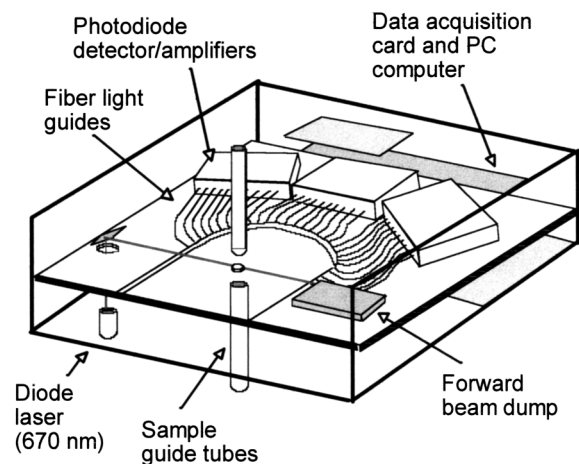


Fig. 1. Layout of the polar nephelometer. Not shown are the three-dimensional light absorbers placed directly above and below the scattering plane. The instrument is enclosed in an aluminum box.

anywhere other than the detector array. The fiber light guides direct the scattered light to 33 large-area silicon photodiode detectors with linear amplifiers that convert the scattered intensities to proportional voltage signals. A data acquisition card and a PC with a solid-state hard drive are mounted in the instrument, allowing one to control, collect, and store the resulting signals. As the instrument uses only 10 W of power, it can be operated with batteries. With the acquisition and averaging of multiple measurements of each channel to reduce electronic noise, the system is capable of linearly measuring over 3 decades of light intensity at 100 full angular measurements per second. The system determines the presence of water or ice particles at the scattering center by monitoring the scattered intensity at the near-forward angles. It automatically stores the measured voltages when this signal increases above an experimentally predetermined level and the signal level measured at the side-scattering angles is above the minimum signal level, as determined by the calibration described below.

The system is calibrated with a 670-nm laser beam directed by a fiber light guide to a small, diffuse Teflon light source, 1.3 cm in diameter, which we constructed to fit at the scattering center and pivot in a manner that allows the source to sweep across the fiber-optic array. When this light source is rotated across the detector array, it simulates an isotropic light source when the strongest detected signal is recovered, and this signal is used to calibrate the detector array via software-implemented multiplicative adjustments in a manner similar to that described in Ref. 9. The relative response between the channels differs by less than 1% at the upper level of the detector sensitivity, and a 10% difference in response is designated as the lower limit of acceptable signal, which provides over 3 decades of response, well within the expected dynamic range of scattering from ice particles and water droplets between the angular detection limits of the instrument. The amount of light scattered into the near-forward detectors from the incident laser beam is minimal and is subtracted from the final scattering results of all experiments.

The system accuracy is verified by measurement of the scattering properties of water droplets generated by a common household ultrasonic humidifier at room temperature (21 °C), as shown in Fig. 2. The water droplets falling through the upper sample tube (which is removed from the instrument and shielded from air currents) are seen as a collimated and continuous white stream of particles. As there are no direct measurements of the droplet-size distribution, several mean effective sizes and variances are generated by Mie calculations and compared with the experimental results. The experimental results are adjusted to fit the normalized theoretical results by use of a multiplicative constant in which a log-normal size distribution with a mean effective radius of 3.75  $\mu\text{m}$  and a variance of 0.1 produces the best match. The error bar of 10% in Fig. 2 represents the system error at the low intensity limit of the instrument's response, whereas the 1% error at the upper end of the instrument's response is not

shown. Overall, the measurement matches the expectation and accurately reproduces the rainbow feature at 140°. The small differences are attributed to errors that are not corrected for by the calibration at the low-intensity range of the instrument response.

The cloud chamber consists of a dry-ice-cooled stainless-steel box with a volume of 0.288 m<sup>3</sup> placed within a larger Styrofoam-insulated plywood box, and an ice cloud is formed by injection of small water drops generated by an ultrasonic humidifier into the cold chamber. Because the chamber walls are directly cooled by the dry ice, there is always a large nucleating surface to produce ice crystals. More information on the ice-cloud properties and the cloud chamber is given in Ref. 10. Placing the nephelometer inside this cloud chamber produces the scattering measurement shown in Fig. 3. The ice crystals falling through the sample tube also appear visually as a collimated and continuous white stream of particles. The ice-crystal habit is determined from photomicrographs of replicas such as that shown at the bottom of Fig. 3, which are formed by the vapor method.<sup>11</sup> Because of the cold temperature of the chamber ( $\cong -30$  °C), small irregular ice crystals with an average mean maximum dimension of  $\sim 7.5$   $\mu\text{m}$  are observed, with a size distribution similar to that described in Ref. 10. The theoretical curve is for randomly oriented irregular bullet rosette and plate crystals with rough surfaces calculated from the unified theory of light scattering by ice crystals<sup>3</sup> using the measured size distribution. The experimental results are matched to the expectations with a multiplicative constant, and the error bar (10%) is determined as described above. As expected for nonspherical particles, there is no indication of a rainbow feature in the reverse direction. The absence of halo phenomena commonly seen at 22° and 46° is an indication of the irregular crystal types generated in the cold chamber. Efforts are under way in the laboratory to generate ice crystals that are more representative of those found in nature.

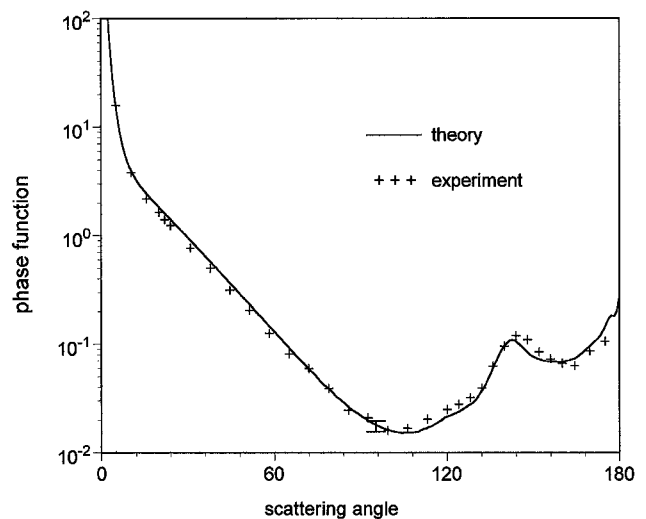


Fig. 2. Experimentally measured two-dimensional scattering properties and the theoretically derived phase function of water droplets with unpolarized incident light.

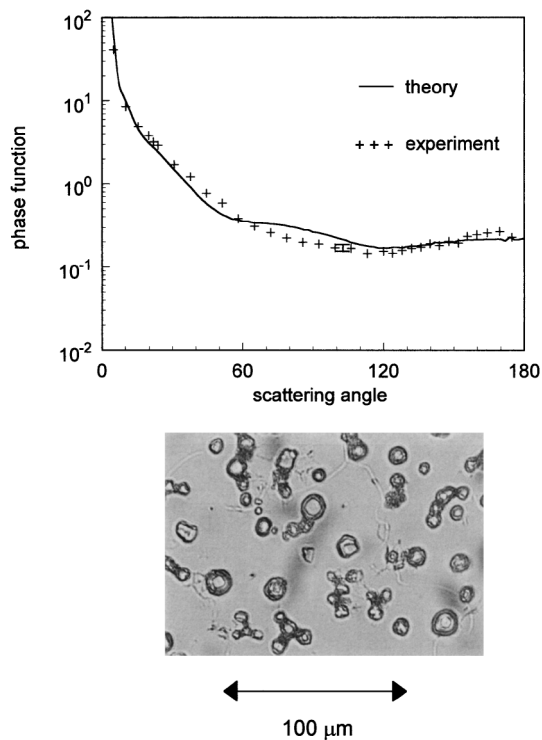


Fig. 3. Top, experimentally measured two-dimensional scattering properties and the theoretically derived phase function of ice crystals with unpolarized incident light. Bottom, photomicrograph of an ice-particle replica taken during the scattering experiment.

We have shown that the measured two-dimensional scattering properties of both laboratory-generated water droplets and ice particles compare well with theoretically derived expectations. We are developing methods to produce scattering measurements of different ice-crystal sizes and shapes in the labora-

tory for further comparison with theoretical results. The instrument reported here is well suited for *in situ* measurements on a balloonborne platform, as it is lightweight and can operate autonomously with batteries. We expect to place this instrument aloft in the near future.

The authors thank W. G. Gellerman and N. Fukuta for their help with the microphysical aspects of this program with regard to the optics and ice and Y. Takano for his assistance with the theoretical calculations. This program was supported by National Science Foundation grant ATM-9907924 and in part by U.S. Air Force Office of Scientific Research grant F499620-98-1-0232. B. Barkey's e-mail address is brian\_barkey@juno.com.

## References

1. Y. Takano and K. N. Liou, *J. Atmos. Sci.* **46**, 3 (1989).
2. Y. Takano and K. N. Liou, *J. Atmos. Sci.* **52**, 818 (1995).
3. K. N. Liou, Y. Takano, and P. Yang, in *Light Scattering by Nonspherical Particles: Theory, Measurements, and Geophysical Applications*, M. I. Mischenko, J. W. Hovenier, and L. D. Travis, eds. (Academic, New York, 2000), pp. 417–449.
4. P. Rolland, K. N. Liou, M. D. King, S. C. Tsay, and G. M. McFarquhar, *J. Geophys. Res.* **105**, 11,721 (2000).
5. K. Sassen and K. N. Liou, *J. Atmos. Sci.* **5**, 838 (1979).
6. P. J. Huffman and W. R. Thursby, *J. Atmos. Sci.* **26**, 1073 (1969).
7. J. F. Gayet, O. Crépel, J. F. Fournol, and S. Oshchepkov, *Ann. Geophys.* **15**, 451 (1997).
8. R. P. Lawson, A. J. Heymsfield, S. Aulenbach, and T. L. Jensen, *Geophys. Res. Lett.* **25**, 1331 (1998).
9. B. Barkey, K. N. Liou, W. Gellerman, and P. Sokolsky, *J. Atmos. Sci.* **56**, 605 (1999).
10. B. Barkey, K. N. Liou, Y. Takano, and W. Gellerman, *Appl. Opt.* **39**, 3561 (2000).
11. T. Takahashi and N. Fukuta, *J. Atmos. Ocean. Technol.* **5**, 129 (1988).